Article

ASP AMERICAN SCIENTIFIC PUBLISHERS

Copyright © 2016 American Scientific Publishers
All rights reserved
Printed in the United States of America

Journal of Nanoscience and Nanotechnology
Vol. 16, 11722–11726, 2016
www.aspbs.com/jnn

Hybrid Metal-Halide Perovskite-MoS_2 Phototransistor

Youngseo Park[1], Sanghyun Lee[1], Hui Joon Park[2], Hyoung Won Baac[3], Geonwook Yoo[4,*], and Junseok Heo[1,*]

[1] *Department of Electrical and Computer Engineering, Ajou University, Suwon 16499, South Korea*
[2] *Division of Energy Systems Research, Ajou University, Suwon 16499, South Korea*
[3] *School of Electronic and Electrical Engineering, Sungkyunkwan University, Suwon 16419, South Korea*
[4] *School of Electronic Engineering, Soongsil University, Seoul 156-743, South Korea*

Two-dimensional (2D) molybdenum disulfide (MoS_2) has attracted much attention as a promising next-generation optoelectronic device. In particular, multilayer MoS_2 has superior optical properties compared to mono- or few-layer MoS_2 because of its higher density of states and wider spectral response. However, as the number of layers increases, multilayer MoS_2 becomes indirect, resulting in poor light absorption and low photoresponsivity. Here, we report the enhanced photocurrent response of a multilayer MoS_2 thin-film transistor by stacking an organometal halide perovskite ($CH_3NH_3PbI_3$) layer on top of the multilyaer MoS_2. With the perovskite overlayer, the photocurrent increased by two orders of magnitude, and thus our proposed hybrid phototransistor exhibited significantly enhanced photoresponsivity of $\sim$1.1 A/W as well as detectivity of $\sim 9 \times 10^{10}$ Jones compared to the MoS_2 phototransistor without the perovskite layer. We also observe that the electrical properties change because of the effect of the overlayer. Our result indicates that multilayer MoS_2 with a $CH_3NH_3PbI_3$ overlayer can be a promising structure for high-performance MoS_2-based photodetector applications.

Delivered by Ingenta to: Dental Library Seoul Natl Univ
IP: 147.46.241.33 On: Tue, 04 Oct 2016 06:16:00
Copyright: American Scientific Publishers

Keywords: MoS_2, Phototransistor, Perovskite, Photoresponsivity, Detectivity.

1. INTRODUCTION

Two-dimensional (2D) transition metal dichalcogenides, in particular MoS_2, have been intensively investigated for applications such as thin-film transistors and photodetectors owing to a large electron mobility, large current ON/OFF ratio, and broad absorption spectrum.[1–7] On the other hand, various physical characteristics have been also studied such as the doping effect, hysteresis, and temperature dependency.[8–13] MoS_2 has a tunable bandgap ranging from 1.2 eV (indirect) to 1.8 eV (direct) according to the number of layers.[5,14] Since the demonstration of an MoS_2 phototransistor with a responsivity of 7.6 mA/W,[15] significant progress has been made, and recently, Lopez-Sanchez et al. reported a very high responsivity of 880 A/W in a single-layer MoS_2 photodetector.[16] Compared with a single-layer MoS_2, multilayer MoS_2 can carry a higher on-current owing to a larger density of states at the minimum conduction band and multiple conducting channels. The thicker MoS_2 layers may also screen the carrier-confined channel region from ambient effects, resulting in enhanced electrical and thermal stability. In spite of these advantages, multilayer MoS_2 becomes an indirect bandgap as the number of layers increases, which is detrimental for optoelectronic applications, resulting in a lower responsivity. In this work, we adopted organometal halide perovskite ($MAPbI_3$) as an additional light-absorbing material. We fabricated the hybrid $MAPbI_3$-MoS_2 phototransistor by spin-coating the synthesized $MAPbI_3$ on the multilayer MoS_2 phototransistor. We have experimentally demonstrated that the hybrid phototransistor has a higher responsivity and detectivity compared with the pristine multilayer MoS_2 phototransistor without the perovskite.

2. EXPERIMENTAL DETAILS

In this work, few layers of MoS_2 were mechanically exfoliated from crystals of bulk MoS_2 (SPI Supplies, USA) using the scotch-tape method, and they were then transferred onto p^{++}Si/SiO_2 (200 nm) substrates. We deposited 20/50 nm Ti/Al on top of the MoS_2 flakes as source and drain electrodes by thermal evaporation using the conventional lift-off technique. The device was then annealed at

*Authors to whom correspondence should be addressed.

1533-4880/2016/16/11722/005 doi:10.1166/jnn.2016.13581

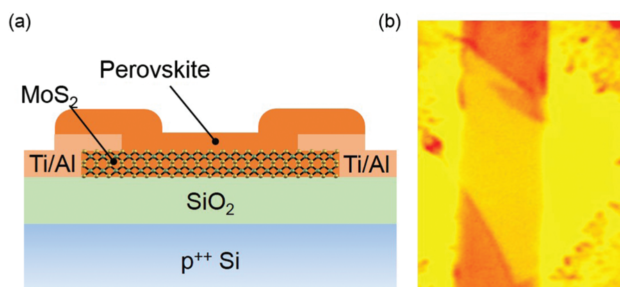

Figure 1. (a) Schematic diagram of fabricated hybrid metal-halide perovskite-MoS_2 phototrasistor. (b) Optical microscope image of the device.

200 °C for 10 min in nitrogen ambient using the rapid thermal process (RTP) to decrease the contact resistance and to remove any organic solvent residues on the MoS_2 surface.[17, 18] We measured the fabricated MoS_2 device to determine its fundamental electrical and optoelectrical properties, after which the thin film of organolead halide perovskite was deposited on the MoS_2 device.

To obtain organolead halide perovskite $CH_3NH_3PbI_3$ ($MAPbI_3$), methylammonium iodide (CH_3NH_3I) was first synthesized by reacting hydroiodic acid (10 ml, 57% in water, Sigma Aldrich) and methylamine (24 ml, 33% in ethanol, Sigma Aldrich) in a 500 mL round bottom flask at 0 °C for 2 h with magnetic stirring. The solution was evaporated at 60 °C for 30 min. After drying, the synthesized chemical was washed three times with ethanol and diethyl ether. Then, the final product of CH_3NH_3I powder was dried at 60 °C for 24 h in vacuum. To prepare 0.4 mol $CH_3NH_3PbI_3$ solution, we mixed methylammonium iodide (synthesized) and PbI_2 (Aldrich) with a molar ratio of 1:1 in a solvent mixture of γ-butyrolactone (GBL) and dimethyl-sulfoxide (DMSO) (7:3 v/v). The $CH_3NH_3PbI_3$ solution was stirred at 70 °C for 12 h.[19]

Figure 1(a) shows the schematic diagram of the hybrid $MAPbI_3$–MoS_2 phototransistor. To increase the wettability of the MoS_2 surface, we applied light oxygen plasma treatment, resulting in a hydrophilic surface on the MoS_2. The $MAPbI_3$ solution was then spin-coated on the top of the MoS_2 device by consecutive two-step processes at 1,000 and 3,000 rpm for 10 and 20 s, respectively. The spin-coated devices were annealed at 100 °C for 10 min in nitrogen ambient, and the expected thickness of the $MAPbI_3$ layer is approximately 60 nm. The optical microscope image of the fabricated device is shown in Figure 1(b). The channel length L and channel width W are approximately 6.5 μm and 11.43 μm, respectively.

3. RESULTS AND DISCUSSION

We measured current–voltage (I–V) characteristics of the MoS_2 phototransistor using a dual-channel source meter (Keithley 2614B) before and after deposition of $MAPbI_3$ in dark conditions to avoid the photo-excitation of carriers. Figures 2(a and b) display the measured transfer (I_{DS}–V_{GS}) characteristics of a pristine MoS_2 phototransistor and hybrid $MAPbI_3$–MoS_2 phototransistors, respectively, which were obtained by sweeping V_{GS} from 30 V to −30 V for $V_{DS} = 0.1$ (black line) and 1 V (red line) at room temperature. We performed all electrical and optical measurements in nitrogen ambient to avoid any possible degradation of the $MAPbI_3$ layer. After spin coating of $MAPbI_3$, the drain current was increased by two orders of magnitude below the threshold voltage, while it decreased above the threshold voltage. These current degradations (higher off-current and low on-current) contributed to the oxidation of the MoS_2 surface during the oxygen plasma treatment.[20] A partial formation of MoO_3 in the MoS_2 channel generates more traps near the interface. As a result, the traps scatter more carriers, leading to a lower on-current, and they simultaneously increase the thermal generation of carriers, contributing to a large off-current. Hence, a surface treatment to convert the wettability of the surface must be applied very gently. Moderated surface treatment techniques such as ultraviolet treatment and laser annealing are under investigation.

Delivered by Ingenta to: Dental Library Seoul Natl Univ
IP: 147.46.211.39 On: Tue, 04 Oct 2016 06:16:00
Copyright: American Scientific Publishers

We estimated the threshold voltages (V_T) using the linear extrapolation method in a linear region. The values are −4.86 and −6.99 V in a pristine MoS_2 phototransistor and hybrid $MAPbI_3$-MoS_2 phototransistor, respectively. In general, the threshold voltage and mobility of 2D materials such as MoS_2 are affected by surface conditions.[21] The negative shift of the threshold voltage after the deposition of $MAPbI_3$ may originate from the electron transfer from $MAPbI_3$ to balance the Fermi levels in equilibrium. The field-effect mobility values (μ_{FE}) of 8.54 and 5.24 cm^2/Vs are also extracted in a pristine MoS_2 phototransistor and a hybrid $MAPbI_3$-MoS_2 phototransistor, respectively, from $\mu_{FE} = L \cdot g_m/(W \cdot C_{OX} \cdot V_{DS})$, where $W/L = 11.43$ μm/6.5 μm, $C_{OX} = 1.7 \times 10^{-8}$ F/cm^2, and $V_{DS} = 1$ V. After the application of $MAPbI_3$ on the MoS_2 layer, the mobility decreased owing to an additional carrier scattering by traps near the MoO_3. The sub-threshold swings (SS) of 2.69 and 3.07 V/dec were estimated from Figures 2(a and b) for a pristine MoS_2 phototransistor and a hybrid $MAPbI_3$-MoS_2 phototransistor, respectively.

Figures 2(c and d) represent the output (I_{DS}–V_{DS}) characteristics of the MoS_2 and hybrid metal-halide $MAPbI_3$-MoS_2 device, respectively, for V_{GS} varying from 0 to 20 V at room temperature. After deposition of $MAPbI_3$ on the MoS_2 surface, the drain current was reduced in the saturation region because of reduced mobility. As previously mentioned, additional surface traps were generated by the application of $MAPbI_3$, which decrease the carrier mobility in the channel. The drain-saturation current ($I_{DS,\,sat}$) of the hybrid $MAPbI_3$–MoS_2 phototransistor slowly increased because of the impact-ionization of carriers after channel pinch-off.

We measured the transfer characteristics of as-fabricated MoS_2 and hybrid perovskite-MoS_2 devices

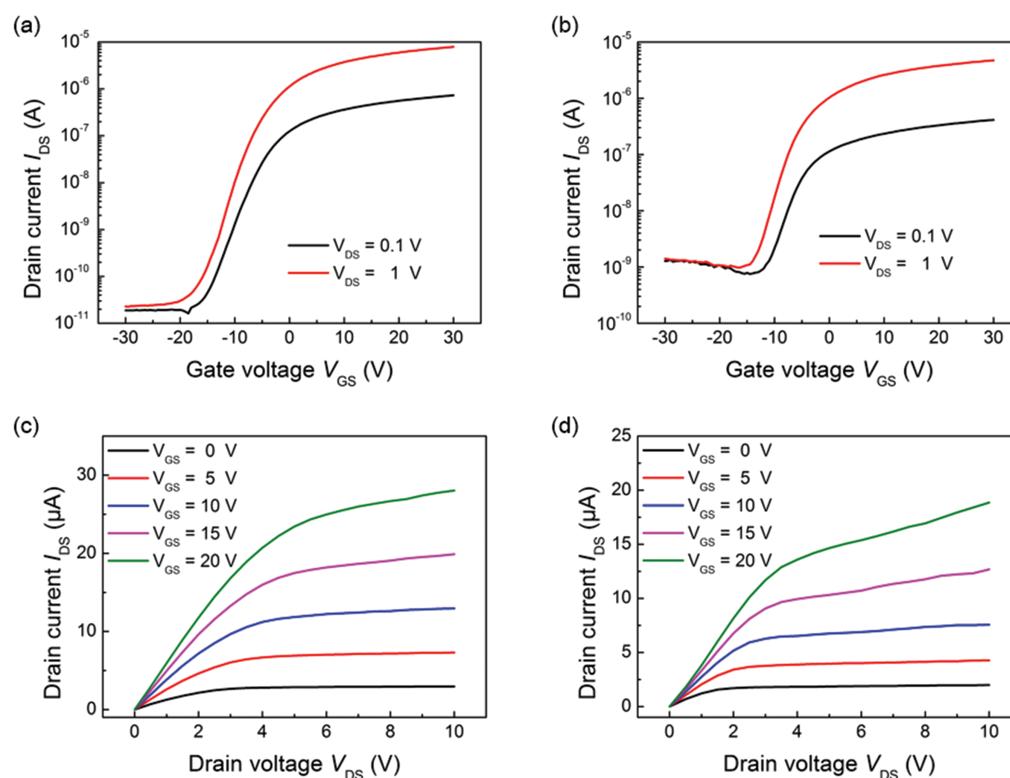

Figure 2. Trasnfer characteristics (I_{DS}–V_{GS}) of (a) MoS_2 and (b) hybrid perovskite-MoS_2 device for 0.1 V (black line) and 1 V (red line) at room temperature in dark condition. Output characteristics (I_{DS}–V_{GS}) of (c) MoS_2 and (d) fabricated device for $V_{GS} = 0$, 5, 10, 15, and 20 V under the same conditions.

Delivered by Ingenta to: Dental Library Seoul Natl Univ
IP: 147.46.241.33 On: Tue, 04 Oct 2016 06:16:00
Copyright: American Scientific Publishers

under illumination for V_{GS} ranging from 30 V to −30 V (backward sweep) with incident power densities of 4, 24, and 50 mW/cm^2 at a wavelength of 638 nm with $V_{DS} = 1$ V (Figs. 3(a and b)). After spin-coating of $MAPbI_3$, I_{DS} increased by two orders of magnitude below the threshold voltage in dark conditions, as described earlier. As the incident power density increased, I_{DS} increased at both devices; we observed a particularly larger current increase in the hybrid $MAPbI_3$-MoS_2 device. A smaller current increase in the pristine MoS_2 device contributed to incomplete light absorption in the thin MoS_2 layer (an absorption coefficient of bulk MoS_2 is approximately 10^5 cm^{-1} at $\lambda = 638$ nm,[22,23] requiring 200–300 nm to absorb all incoming light). On the other hand, in the hybrid $MAPbI_3$–MoS_2, light is also absorbed by the perovskite ($MAPbI_3$) layer, where photogenerated electrons and holes are transported into the MoS_2 layer, resulting in a larger current increase.

Figures 4(a and b) show the extracted photo current ($I_{ph} = I_{DS}$–I_{dark}) along the dark current (I_{dark}) as a function of the gate voltage for various optical power densities (4, 24, and 50 mW/cm^2) in the pristine MoS_2 and the

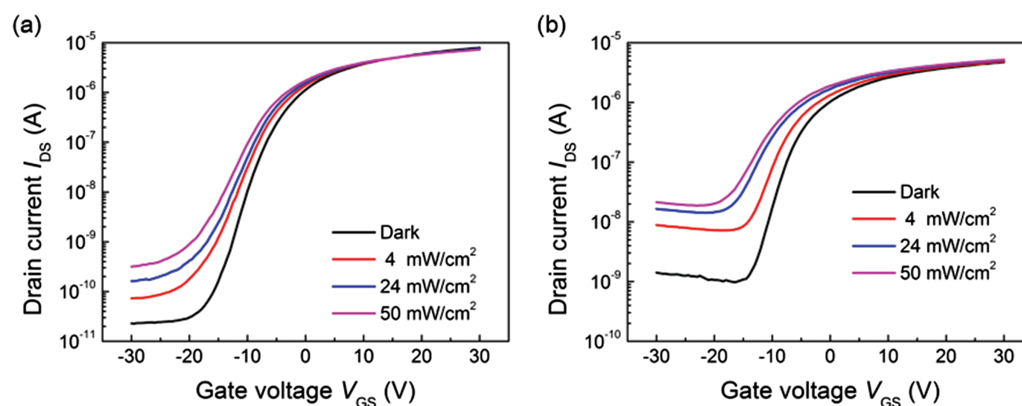

Figure 3. Transfer characteristics (I_{DS}–V_{GS}) of (a) MoS_2 and (b) hybrid metal-halide perovskite-MoS_2 device with incident light for various power densities (4, 24, and 50 mW/cm^2) at $V_{DS} = 1$ V. The incident laser wavelength is 638 nm.

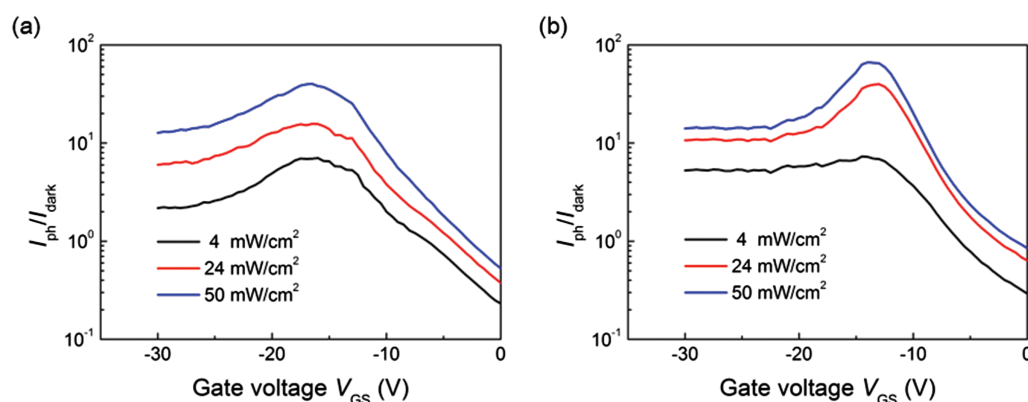

Figure 4. Extracted photocurrent ($I_{ph} = I_{DS}-I_{dark}$) along the dark current as a function of the gate voltage of (a) MoS_2 and (b) hybrid perovskite-MoS_2 devices for various power densities (4, 24, and 50 mW/cm²) under the same conditions.

hybrid $MAPbI_3$-MoS_2 device, respectively. Overall, these contrasts were highest around −17 to −13 V, and they decreased with increased gate bias. The stronger transverse electric field was applied at the channel with increased gate bias, reducing the carrier mobility of photogenerated carriers in the channel. As a result, I_{ph} decreased at a large negative gate bias. When the gate bias increases, electron accumulation in the channel increases the dark current; hence, the contrast decreases again. A low dark current in the pristine MoS_2 may be good for detecting low-level light, but the I_{ph}/I_{dark} contrast was worse for a weak optical power density (4 mW/cm²) compared to the hybrid device. The contrast in the hybrid $MAPbI_3$-MoS_2 structure was from 5 to 7 for any gate voltage, and was always higher than that of the pristine device.

We calculated the responsivity (R) of the pristine MoS_2 and the hybrid $MAIPbI_3$–MoS_2 using $R = I_{ph}/P_{inc}$, where P_{inc} is the incident optical power, as shown in Figure 5. When V_{GS} increases close to the threshold voltage, the responsivity is generally highest, and the maximum responsivity corresponds to an external quantum efficiency of more than 100%. We estimated the gain mechanism using the carrier's asymmetric mobility and transport. The photogenerated electrons are swept faster than holes, and the remaining holes may induce more electrons from the source to the channel. The responsivity of the hybrid $MAPbI_3$-MoS_2 structure was greater by a maximum of two orders of magnitude compared to the pristine MoS_2 structure when the gate bias was less than −10 V. Note that for a gate bias larger than 10 V, the contrast of I_{ph}/I_{dark} is not sufficient, and I_{ph} will not be easily separated from the dark current.

Figure 6 displays the responsivity and specific detectivity (D^*) of the variable P_{inc} (4, 24, and 50 mW/cm²) and $V_{GS} = -20$ V. The specific detectivity refers to the detector sensitivity. If the major contributor to the total current is the shot noise at dark current, it is given as $D^* = RA^{1/2}/(2qI_{dark})^{1/2}$, where R is the responsivity, A is the area of the detector, q is the unit charge, and I_{dark} is the dark current.[24] After the application of $MAPbI_3$ on the MoS_2 layer, the specific detectivity also increased by one order of magnitude at variable incident optical power, and this was due to the photocurrent absorbed from the $MAPbI_3$ layer. If the MoS_2 treatment method is improved for the reduction of the dark current, the specific detectivity will be further improved.

Delivered by Ingenta to: Dental Library Seoul Nat'l Univ
Copyright: American Scientific Publishers

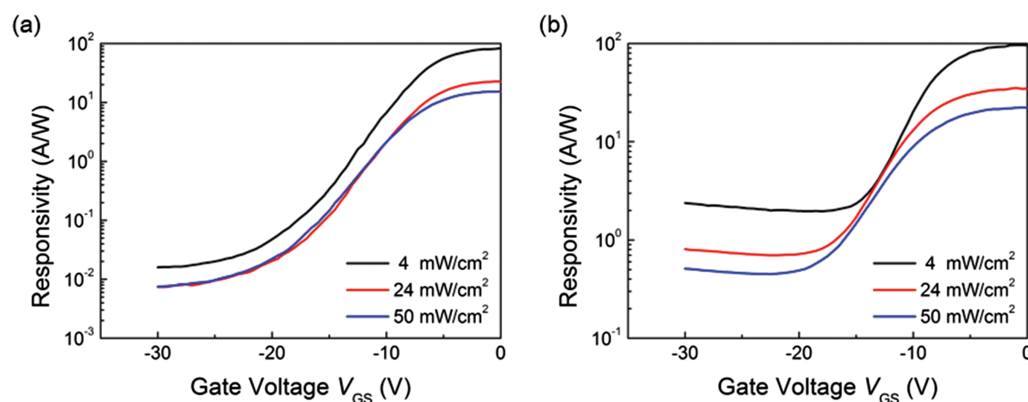

Figure 5. Aa responsivity ($R = I_{ph}/P_{inc}$, where P_{inc} is the incident optical power) as a function of the gate voltage of (a) MoS_2 and (b) hybrid perovskite-MoS_2 devices. The laser wavelength is 638 nm with various power densities (4, 24, and 50 mW/cm²).

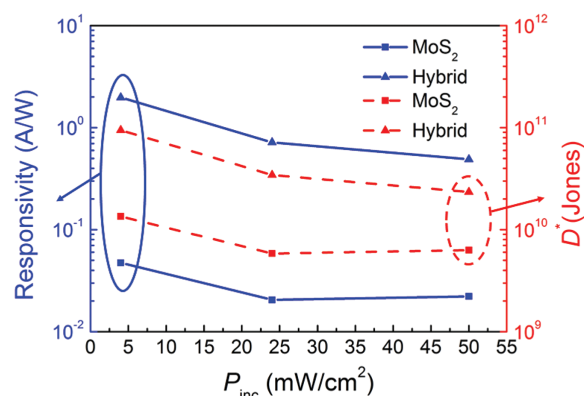

Figure 6. Aa responsivity (R) and specific detectivity (D^*) as a function of the variable P_{inc} (4, 24, and 50 mW/cm^2) with a laser wavelength of 638 nm.

4. CONCLUSION

In conclusion, we have fabricated hybrid organometal halide perovskite-MoS_2 phototransistors and characterized their electrical and optical properties. We also characterized the MoS_2 thin-film transistors as a control sample before the deposition of perovskite. We observed that the threshold voltage shifts negatively and the mobility degrades after the perovskite was applied. The MoS_2 phototransistor coated with perovskite exhibits a larger dark current, but has a wider range of gate voltage bias for which the photocurrent is larger than the dark current. Moreover, the hybrid phototransistors showed a larger responsivity and detectivity compared to the MoS_2 phototransistor. Therefore, by using the perovskite layer as an additional light-absorbing layer, we improve the photodetection in MoS_2 phototransistors, and this hybrid scheme can compensate for the relatively poor absorption in few-layer MoS_2 with an indirect bandgap.

Acknowledgment: This research was supported by the Basic Science Research Program through the National Research Foundation of Korea (NRF) funded by the Ministry of Science, ICT and Future Planning (MSIP) (NRF-2013R1A1A1058044), and by the NRF grant funded by the MSIP (No. NRF-2015M2B2A9033138). This work was also supported by the Ministry of Trade, Industry and Energy (MOTIE, 10051565) and Korea Display Research Corporation (KDRC) support program for the development of future devices technology for display industry.

References and Notes

1. M. Chhowalla, H. S. Shin, G. Eda, L.-J. Li, K. P. Loh, and H. Zhang, *Nat. Chem.* 5, 263 (**2013**).
2. Q. H. Wang, K. Kalantar-Zadeh, A. Kis, J. N. Coleman, and M. S. Strano, *Nat. Nanotechnol.* 7, 699 (**2012**).
3. K. F. Mak, C. Lee, J. Hone, J. Shan, and T. F. Heinz, *Phy. Rev. Lett.* 105, 136805 (**2010**).
4. A. Splendiani, L. Sun, Y. Zhang, T. Li, J. Kim, C.-Y. Chim, G. Galli, and F. Wang, *Nano Lett.* 10, 1271 (**2010**).
5. B. Radisavljevic, A. Radenovic, J. Brivio, V. Giacometti, and A. Kis, *Nat. Nanotechnol.* 6, 147 (**2011**).
6. H. Wang, L. Yu, Y.-H. Lee, Y. Shi, A. Hsu, M. L. Chin, L.-J. Li, M. Dubey, J. Kong, and T. Palacios, *Nano Lett.* 12, 4674 (**2012**).
7. C. Chen, H. Qiao, S. Lin, C. M. Luk, Y. Liu, Z. Xu, J. Song, Y. Xue, D. Li, J. Yuan, W. Yu, C. Pan, S. P. Lau, and Q. Bao, *Sci. Rep.* 5, 11830 (**2015**).
8. S. Sahoo, A. P. S. Gaur, M. Ahmadi, M. J.-F. Guinel, and R. S. Katiyar, *J. Phys. Chem. C* 117, 9042 (**2013**).
9. T. Korn, S. Heydrich, M. Hirmer, J. Schmutzler, and C. Schüller, *Appl. Phys. Lett.* 99, 102109 (**2011**).
10. L. Yang, K. Majumdar, H. Liu, Y. Du, H. Wu, M. Hatzistergos, P. Y. Hung, R. Tieckelmann, W. Tsai, C. Hobbs, and P. D. Ye, *Nano Lett.* 14, 6275 (**2014**).
11. Y. Park, H. W. Baac, J. Heo, and G. Yoo, *Appl. Phys. Lett.* 108, 083102 (**2016**).
12. D. Kufer and G. Konstantatos, *Adv. Mater.* 27, 176 (**2015**).
13. Y. Guo, X. Wei, J. Shu, B. Liu, J. Yin, C. Guan, Y. Han, S. Gao, and Q. Chen, *Appl. Phys. Lett.* 106, 103109 (**2015**).
14. L. Liu, S. B. Kumar, Y. Ouyang, and J. Guo, *IEEE Trans. Electron Devices* 58, 3042 (**2011**).
15. Z. Yin, H. Li, H. Li, L. Jiang, Y. Shi, Y. Sun, G. Lu, Q. Zhang, X. Chen, and H. Zhang, *ACS Nano* 6, 74 (**2011**).
16. O. Lopez-Sanchez, D. Lembke, M. Kayci, A. Radenovic, and A. Kis, *Nat. Nanotechnol.* 8, 497 (**2013**).
17. J. Kwon, Y. K. Hong, G. Han, I. Omkaram, W. Choi, S. Kim, and Y. Yoon, *Adv. Mater.* 27, 2224 (**2015**).
18. S. Kim, A. Konar, W.-S. Hwang, J. H. Lee, J. Lee, J. Yang, C. Jung, H. Kim, J.-B. Yoo, J.-Y. Choi, Y. W. Jin, S. Y. Lee, D. Jena, W. Choi, and K. Kim, *Nat. Commun.* 3, 1011 (**2012**).
19. Y. Xu, L. Zhu, J. Shi, X. Xu, J. Xiao, J. Dong, H. Wu, Y. Luo, D. Li, Q. Meng, *ChemPhysChem.* 17, 112 (**2016**).
20. M. R. Islam, N. Kang, U. Bhanu, H. P. Paudel, M. Erementchouk, L. Tetard, M. N. Leuenberger, and S. I. Khondaker, *Nanoscale* 6, 10033 (**2014**).
21. D. J. Late, B. Liu, H. S. S. R. Matte, V. P. Dravid, and C. N. R. Rao, *ACS Nano.* 6, 5635 (**2012**).
22. X. Yan, L. Zhu, Y. Zhou, Y. E, L. Wang, and X. Xu, *Appl. Opt.* 54, 6732 (**2015**).
23. M. Bernardi, M. Palummo, and J. C. Grossman, *Nano Lett.* 13, 3664 (**2013**).
24. W. Choi, Y. M. Cho, A. Konar, J. H. Lee, G. B. Cha, S. C. Hong, and J. Joo, *Adv. Mater.* 24, 5832 (**2012**).

Delivered by Ingenta to: Dental Library Seoul Nat'l Univ
IP: 147.46.241.33 On: Tue, 04 Oct 2016 06:18:00
Copyright: American Scientific Publishers

Received: 31 March 2016. Accepted: 29 June 2016.